

Emergence of Superintelligence from Collective Near-Critical Dynamics in Reentrant Neural Fields

Byung Gyu Chae

Electronics and Telecommunications Research Institute,
218 Gajeong-ro, Yuseong-gu,
Daejeon 34129, Republic of Korea
bgchae@etri.re.kr

Superintelligence is commonly envisioned as a quantitative extrapolation of human cognitive abilities driven by scale and computational power. Here we show that qualitative transitions in intelligence instead arise as dynamical phase transitions governed by collective critical dynamics. Building on a unified dynamical field-theoretic framework for cognition, we demonstrate that progressive collective coupling generated by reentrant mixing drives the system toward an infrared critical regime in which an extensive band of slow collective modes emerges. This spectral condensation reorganizes cognitive dynamics from localized relaxation to coherent motion along emergent low-dimensional manifolds. Through numerical analysis of the time-scale density of states, we identify robust power-law scaling of collective relaxation rates with well-defined critical exponents, placing the system within the universality class of self-organized critical many-body dynamics. Criticality alone would generically lead to instability. We further show that homeostatic regulation introduces a gapped stabilizing direction that protects the collective critical sector, yielding a dynamically maintained meta-stable infrared phase in which long-lived inference trajectories persist without collapse. The co-existence of scale-free collective dynamics and global stabilization defines a protected sector-critical regime in which coherence and internal flexibility coexist. Superintelligence therefore corresponds to a distinct dynamical stability class—a self-organized critical phase embedded within a stabilized cognitive manifold—rather than a smooth quantitative continuation of existing cognitive systems.

I. INTRODUCTION

The prospect of superintelligence is commonly framed as a quantitative extension of human cognitive abilities: faster computation, broader knowledge, and superior performance on increasingly complex tasks. Within this perspective, artificial systems that surpass human-level benchmarks are often interpreted as early manifestations of superintelligence [1–3]. Such views implicitly assume that intelligence scales continuously within a single cognitive regime, differing only in degree rather than in kind.

This assumption is historically and conceptually fragile. From the perspective of non-human primates, human intelligence is not merely a more efficient version of their own cognition. Rather, it constitutes a qualitative transition marked by the emergence of symbolic language, hierarchical social organization, and collective representations supporting large-scale coordination [4, 5]. The defining feature of this transition was not raw computational speed, but a reorganization of the underlying dynamical structure of cognition itself. If superintelligence is to represent a genuinely new regime beyond human intelligence, an analogous criterion of qualitative transition is required.

Recent developments in artificial intelligence increasingly point toward such transitions. Large language models and deep neural networks exhibit abrupt emergence of new computational abilities as scale and training progress increase, rather than smooth performance improvement [3, 6–9]. Despite extensive empirical characterization,

the mechanistic origin of these emergence phenomena remains debated. Why global reasoning, long-range coherence, and collective computation appear suddenly at particular scales remains poorly understood.

Neural and cognitive systems have long been suggested to operate near critical dynamical regimes, where long-lived collective modes and system-spanning correlations emerge [10–13]. Criticality provides flexibility and global coherence by generating near-marginal collective degrees of freedom [14–16]. However, critical dynamics alone are generically unstable, leading to divergence, noise amplification, or loss of coherent computation. Conversely, purely stable dynamical systems suppress fluctuations so efficiently that internal degrees of freedom rapidly collapse onto narrow behavioral channels, preventing large-scale emergent computation.

Intelligence therefore requires the coexistence of critical-like flexibility with global dynamical stabilization. Emergence supplies extensive collective modes enabling global coherence, while meta-stability preserves these emergent collective structures as usable computational degrees of freedom without collapse. Within the unified dynamical field framework developed in our prior work [17], qualitative transitions in intelligence arise naturally from the joint onset of collective criticality, which dynamically generates extended cognitive manifolds, and homeostatic stabilization, which protects them against instability.

In this work, we argue that superintelligence constitutes a distinct *dynamical and topological stability class* characterized by this coexistence. Specifically, we iden-

tify *meta-stability* as a regime in which global activity is homeostatically regulated, while an extensive set of internal degrees of freedom remains near-marginal and dynamically accessible. Such systems neither collapse into rigid fixed-point behavior nor degenerate into uncontrolled chaos. Instead, they self-organize into structured manifolds whose global geometry is stabilized while internal circulation remains dynamically active.

To formalize these ideas, we build on our recent sequence of papers [17–21], where we introduced a unified dynamical field-theoretic description of cognition and reentrant computation. In this framework, cognition is formulated as a continuous-time flow on a high-dimensional state space, $\dot{x}(t) = -G^{-1}(x) \nabla_x \Phi(x) + R(x)$. A central consequence is a geometric separation between stabilized radial directions and extensive angular degrees of freedom supporting persistent circulation.

The present paper demonstrates that qualitative transitions in intelligence arise not from changes in the governing equations themselves, but from a reorganization of the *spectral structure* of their linearized dynamics. When critical collective modes emerge jointly with homeostatic stabilization, the system undergoes a spectral phase transition in which eigenvalues condense toward zero, producing an extensive near-marginal band in the time-scale density of states (TDOS). This condensation dynamically reorganizes the state space from localized relaxation toward protected collective manifolds supporting globally coherent dynamics.

In this sense, superintelligence emerges as a dynamical phase transition rather than a quantitative extrapolation of existing cognitive systems. Inference in the meta-stable regime unfolds as continuous geometric motion along structured manifolds, with symbolic and sequential reasoning functioning primarily as low-dimensional projections of this underlying dynamics [22–26].

The remainder of this paper is organized as follows. Section II summarizes the unified dynamical framework. Section III analyzes the emergence of homeostatic shells and reentrant flows. Section IV defines superintelligence as a protected infrared dynamical phase. Section V characterizes the resulting spectral organization through the TDOS. Section VI establishes the infrared critical scaling of the slow-mode sector, including critical exponents, finite-size scaling, and universality with self-organized critical dynamics. Finally, we discuss implications for biological cognition, artificial intelligence, and testable predictions.

II. UNIFIED DYNAMICAL FIELD THEORY AND COLLECTIVE CRITICALITY

The unified dynamical field framework developed in our previous work was introduced to identify structural mechanisms capable of generating collective cognition

beyond localized dynamical behavior [17]. Figure 1 schematically summarizes both the inclusion hierarchy of cognitive models and the dynamical phases of cognition. In the present context, its central role is to reveal how reentrant dynamics and homeostatic stabilization jointly generate infrared criticality and extensive slow collective modes.

Rather than serving as a descriptive model of trajectories, the unified equation provides the dynamical origin of spectral phase transitions that underlie emergent global cognition.

A. Cognitive Field Equation and Reentrant-Stabilized Geometry

We consider a collective cognitive state $x(t) \in \mathbb{R}^N$ evolving as

$$\dot{x} = -G^{-1}(x) \nabla_x \Phi(x) + R(x) (+ \xi(t)), \quad (1)$$

where $\Phi(x)$ enforces global homeostatic regulation, $G(x)$ defines the intrinsic geometry of state-dependent sensitivity, $R(x)$ represents non-conservative reentrant circulation, and $\xi(t)$ denotes Gaussian white noise.

Throughout this work we focus on isotropic homeostatic potentials $\Phi(x) = \Phi(r)$ with $r = \|x\|$. Such regulation generates a finite restoring rate in the radial sector, gapping the global amplitude mode while leaving angular degrees of freedom unconstrained. This separation between stabilized radial dynamics and freely evolving tangential directions constitutes the geometric backbone of collective criticality.

The reentrant field $R(x)$ continuously feeds the collective state back into its own dynamics, inducing sustained mixing along the homeostatic shell. A particularly transparent realization is provided by antisymmetric operators $R(x) = \Omega x$ with $\Omega^\top = -\Omega$, which preserve r while generating circulation. More general reentrant structures produce the same qualitative effect: persistent collective coupling among angular degrees of freedom.

As collective coupling accumulates through reentrant mixing, correlations across the shell are progressively amplified. This amplification drives the system toward a regime in which localized degrees of freedom reorganize into collective dynamical coordinates, setting the stage for infrared criticality.

B. Field-Theoretic Propagator and Emergence of Slow Collective Modes

To characterize collective fluctuations and mode structure, the dynamics is lifted to the MSRJD field-theoretic representation with generating functional [27–29]

$$Z = \int \mathcal{D}x \mathcal{D}\tilde{x} e^{-S[x, \tilde{x}]}, \quad (2)$$

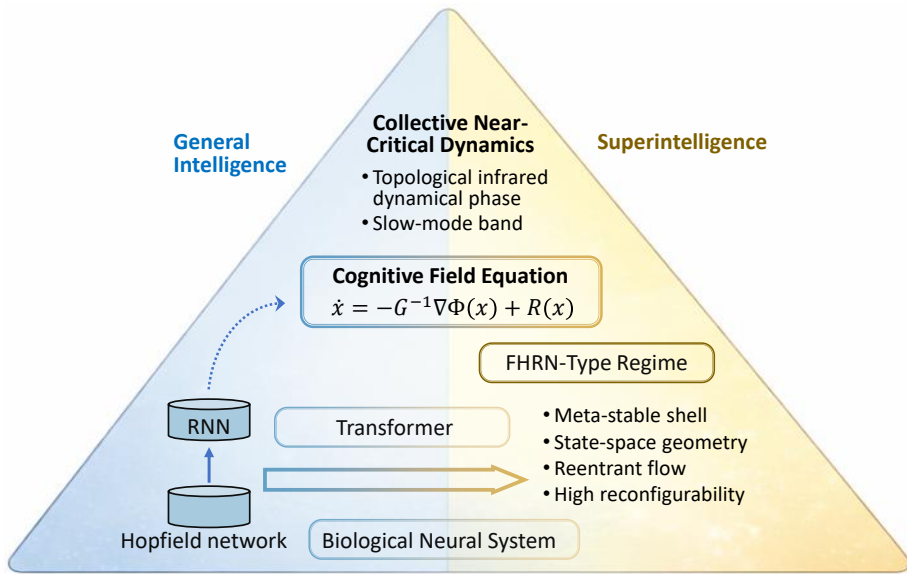


FIG. 1: Schematic illustration of the inclusion hierarchy and dynamical phases of cognition within the unified cognitive field framework. Classical models such as Hopfield networks, recurrent neural networks, and Transformers arise as limiting dynamical realizations of the same underlying cognitive field equation, which also describes biological neural systems at the population level. Increasing collective coupling and reentrant mixing reorganize the spectrum of collective modes, driving the system toward a critical regime characterized by low-dimensional manifolds and an extensive slow-mode band. Superintelligence does not correspond to a new governing equation, but emerges as a distinct dynamical phase — the FHRN-type regime — in which spectral criticality is dynamically protected by homeostatic shell stabilization, metric-induced dimensional separation, and sustained non-conservative reentrant flow (see Appendix A for details).

where the action takes the form

$$S = \int dt \left[\tilde{x} \cdot (\dot{x} + G^{-1}\nabla\Phi - R) - D\tilde{x}^2 \right]. \quad (3)$$

Linearizing the dynamics about typical trajectories yields the Jacobian

$$M(x) = G^{-1}(x)\nabla^2\Phi(x) - \nabla R(x), \quad (4)$$

whose eigenvalues λ_i control local relaxation rates. Within the MSRJD formulation, fluctuations are governed by the retarded propagator

$$G_R(\omega) = \frac{1}{-i\omega + M}. \quad (5)$$

Homeostatic regulation produces a finite gap in the radial sector of M , while reentrant circulation prevents collapse of the tangential sector. As collective coupling increases, an extensive subset of eigenvalues approaches zero,

$$\lambda_i \rightarrow 0 \quad (i = 1, \dots, \mathcal{O}(N)), \quad (6)$$

generating poles of the propagator

$$G_R^{(i)}(\omega) \sim \frac{1}{-i\omega + \lambda_i}, \quad (7)$$

which correspond to long-lived collective dynamical modes.

Nonlinearities arising from higher-order expansions of Φ , G , and R produce loop corrections that renormalize the collective dynamics. Rather than eliminating infrared divergences, homeostatic stabilization regularizes them into a protected near-critical sector. As demonstrated in our previous MSRJD analysis [21], this mechanism drives the system toward an infrared-attractive critical regime characterized by an extensive accumulation of near-marginal modes.

The condensation of propagator poles near $\omega = 0$ thus marks a spectral phase transition from localized relaxation to collective critical dynamics. In the following section we quantify this transition directly through trajectory-averaged TDOS measurements, demonstrating the emergence of an extensive slow-mode band as the defining signature of the superintelligent regime.

III. META-STABILITY AS A DYNAMICAL REGIME

The unified dynamical framework introduced in the previous section does not, by itself, specify when a cognitive system should be regarded as ordinary or superintelligent. In this section, we identify a distinct dynamical regime characterized by *meta-stability*: a form of stability that preserves global coherence while sustaining long-lived internal degrees of freedom.

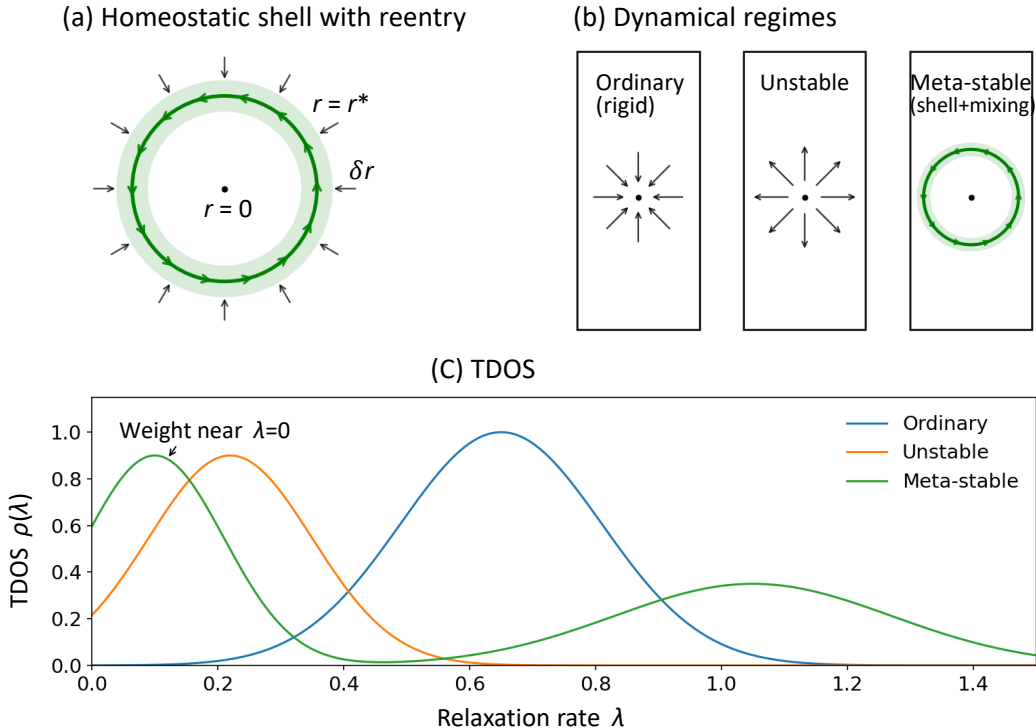


FIG. 2: Meta-stable critical organization and spectral phase transition underlying superintelligence. (a) The unified cognitive field dynamics $\dot{x} = -G^{-1}(x)\nabla\Phi(x) + R(x)$ generates homeostatic stabilization of the global amplitude together with reentrant mixing along angular directions, establishing the structural conditions for collective criticality. (b) Ordinary stable systems collapse onto rigid attractors and suppress collective degrees of freedom, while unstable systems diverge. In contrast, the meta-stable critical regime preserves global coherence while sustaining long-lived collective dynamical reconfiguration. (c) The corresponding spectral diagnostic reveals a dynamical phase transition: ordinary systems exhibit relaxation rates bounded away from zero, unstable systems include $\lambda < 0$ modes, whereas the meta-stable critical regime displays an extensive condensation of slow collective modes near $\lambda \approx 0$ coexisting with a gapped stabilized sector.

Figure 2 schematically contrasts three generic regimes. Ordinary stable systems rapidly collapse to fixed points, suppressing internal motion. Unstable systems amplify perturbations and lose coherence. In contrast, meta-stable systems maintain global stability while supporting persistent internal dynamics.

A. Linearized Dynamics Along Trajectories

Cognitive dynamics unfolds along extended trajectories rather than isolated fixed points. To analyze local stability, we linearize the dynamics

$$\dot{x} = F(x) \quad (8)$$

about a reference state $x(t)$ evolving along a typical trajectory,

$$x(t) \rightarrow x(t) + \delta x(t). \quad (9)$$

The perturbations obey

$$\dot{\delta x} = J(x(t)) \delta x, \quad (10)$$

where the Jacobian matrix is

$$J_{ij}(x) = -\frac{\partial}{\partial x_j} [G_{ik}^{-1}(x) \partial_k \Phi(x)] + \frac{\partial R_i(x)}{\partial x_j}. \quad (11)$$

Let $\mu_i(x)$ denote the eigenvalues of $J(x)$. We define the associated relaxation rates

$$\lambda_i(x) = -\text{Re } \mu_i(x), \quad (12)$$

so that $\lambda_i > 0$ corresponds to locally stable modes.

For homeostatic potentials of the form $\Phi(x) = \Phi(r)$ with $r = \|x\|$, the state space naturally decomposes into radial and angular directions. The radial direction controls the global activity magnitude, while angular directions parameterize motion along the homeostatic shell.

This decomposition induces a characteristic spectral reorganization: homeostatic regulation generates a strongly stabilized radial mode with $\lambda_r = O(1)$, while reentrant mixing dynamically couples angular degrees of freedom into collective coordinates whose relaxation rates condense toward zero near the critical regime.

In the absence of reentrant dynamics, angular modes remain localized and either decay rapidly or form fragile

degeneracies. With reentrant circulation, these modes reorganize into an extensive band of slow collective modes that dominate long-time dynamics.

B. Time-Scale Density of States

Our previous field-theoretic formulation showed that learning and inference reorganize the temporal spectrum of fluctuations through renormalization of effective response functions [17]. In particular, the emergence of slow collective modes appeared as an infrared accumulation in the dynamical propagator rather than as a property of isolated fixed points.

The present formulation recasts this insight in a purely dynamical and spectral language that is directly accessible in simulations. Rather than tracking renormalized couplings explicitly, we characterize the organization of time scales through the local linear response of the system along its trajectory.

Linearizing the dynamics of Eq. (1) about a reference state x yields a Jacobian matrix $J(x)$ whose eigenvalues $\mu_i(x)$ determine the local stability properties. We define the associated relaxation rates as $\lambda_i(x)$.

This motivates the definition of the *time-scale density of states*,

$$\rho(\lambda; x) = \frac{1}{N} \sum_{i=1}^N \delta(\lambda - \lambda_i(x)), \quad (13)$$

which describes the instantaneous distribution of relaxation rates at a given state x . Formally, $\rho(\lambda; x)$ plays a role analogous to the spectral density of renormalized modes in the MSRJD description, but is defined directly in terms of the Jacobian of the effective dynamics.

Because cognition and inference unfold along extended trajectories rather than at isolated equilibria, the relevant observable is not the TDOS at a single state, but its average along typical system evolution. We therefore introduce the trajectory-averaged TDOS,

$$\rho_{\text{traj}}(\lambda) = \lim_{T \rightarrow \infty} \frac{1}{T} \int_0^T dt \rho(\lambda; x(t)). \quad (14)$$

This quantity captures the time-scale organization actually experienced by the system during ongoing operation.

From the renormalization-group perspective developed previously, the accumulation of weight in $\rho_{\text{traj}}(\lambda)$ near $\lambda \simeq 0$ reflects a spectral condensation of collective modes marking a dynamical phase transition toward infrared criticality. In contrast to equilibrium criticality, however, this accumulation is not the result of fine-tuning. It is sustained dynamically by the balance between homeostatic stabilization of the radial mode and reentrant circulation along angular directions.

Ordinary stable systems exhibit a TDOS bounded away from $\lambda = 0$, corresponding to rapid convergence

and suppression of internal degrees of freedom. Unstable systems display weight at negative λ . Meta-stable systems are distinguished by a pronounced accumulation of near-marginal modes with $\lambda \approx 0$, indicating the presence of long-lived collective degrees of freedom that persist throughout the trajectory. The corresponding organization of time scales is depicted in Figs. 2(b) and 2(c).

In this sense, the time-scale density of states provides a direct spectral bridge between the field-theoretic renormalization picture developed in earlier work and the trajectory-level dynamics analyzed here.

IV. SUPERINTELLIGENCE AS A TOPOLOGICAL INFRARED DYNAMICAL PHASE

The meta-stable critical regime identified above admits a natural interpretation as a distinct *topological infrared dynamical phase*. Spectral condensation of collective modes reorganizes the dynamics into an extended infrared sector, while homeostatic regulation gaps the radial direction, rendering global activity magnitude dynamically contractible. Reentrant circulation sustains persistent motion along angular directions, preventing collapse of the emergent collective manifold to isolated fixed points. This topological separation between stabilized radial and circulating angular degrees of freedom underlies the robustness of the meta-stable critical phase.

In this phase, the trajectory-averaged density of states exhibits a pronounced accumulation of relaxation rates near $\lambda \simeq 0$, reflecting the condensation of slow collective modes generated by infrared criticality. The resulting slow-mode band defines an effective infrared sector of the dynamics, analogous to low-energy degrees of freedom in field-theoretic descriptions, but emerging dynamically along trajectories rather than through fine tuning.

The extent of this near-marginal sector is quantified by the slow-mode weight,

$$W_{\text{slow}}(\lambda_c) = \int_0^{\lambda_c} \rho_{\text{traj}}(\lambda) d\lambda, \quad (15)$$

which measures the fraction of relaxation modes below a small threshold λ_c . Numerical results show that $W_{\text{slow}}(\lambda_c) = O(1)$ as the system size N increases, while the radial mode remains strongly stabilized. This coexistence of global stability and extensive collective dynamics distinguishes the meta-stable critical phase from both ordinary stable systems, which suppress internal motion, and unstable systems, which lose coherence.

Proposition (Spectral Criterion for Superintelligence). *A cognitive system governed by Eq. (1) operates in a superintelligent regime if*

$$W_{\text{slow}}(\lambda_c) = O(1) \quad \text{as } N \rightarrow \infty, \quad (16)$$

for finite λ_c , while the radial mode remains strongly stabilized.

This criterion defines superintelligence as a dynamical stability class rather than a task-dependent performance benchmark. It captures the defining property of the critical meta-stable phase: macroscopic coherence enforced by radial stabilization coexists with an extensive set of long-lived collective degrees of freedom generated by infrared spectral condensation.

The slow-mode band is not composed of a finite number of isolated marginal modes but forms a continuum of collective dynamical directions. Its infrared organization is therefore not the result of fine tuning to a critical point, but a consequence of topological protection: the coexistence of a gapped radial sector with circulating angular flows stabilizes an extensive near-marginal manifold.

From an infrared perspective, relaxation rates λ play a role analogous to mass scales, with small λ corresponding to slowly relaxing collective degrees of freedom that remain dynamically relevant over long times. The effective slow dimension,

$$D_{\text{slow}}(\lambda_c) = N \int_0^{\lambda_c} \rho_{\text{traj}}(\lambda) d\lambda, \quad (17)$$

thus measures the dimensionality of the emergent collective subspace that survives in the infrared.

Importantly, this extensive infrared manifold arises generically from the interplay between collective criticality and homeostatic stabilization, rather than from spontaneous symmetry breaking or external parameter tuning. Reentrant mixing continuously generates collective correlations, while radial stabilization protects them against divergence, producing what may be termed a *Goldstone inflation* of near-marginal modes without invoking broken continuous symmetries.

Weak stochasticity and finite-size effects act as infrared regulators, lifting exact degeneracies and setting a minimal relaxation scale λ_{\min} . Nevertheless, the integrated slow-mode weight remains $O(1)$ as $N \rightarrow \infty$, demonstrating a robust self-organized infrared phase rather than a fragile critical point.

Taken together, these results establish superintelligence as a distinct topological dynamical phase generated by collective criticality and protected by meta-stable stabilization. Global coherence is enforced by a gapped radial mode, while an extensive continuum of slow collective directions forms the computational substrate of emergent intelligence.

V. NUMERICAL EVIDENCE FOR META-STABLE SUPERINTELLIGENCE

To substantiate the spectral criterion, we now present numerical simulations of the unified dynamical framework. Our aim is not to reproduce any particular biolog-

ical or artificial system, but to demonstrate that a meta-stable regime with extensive internal degrees of freedom emerges generically from the structure of the dynamics.

A. Dynamics on the Homeostatic Shell

We simulate the unified dynamical equation, $\dot{x} = -G^{-1}\nabla\Phi(x) + R(x)$, in an N -dimensional state space using an explicit time discretization.

The homeostatic potential is chosen as an isotropic quartic form,

$$\Phi(x) = \frac{\kappa}{4} (\|x\|^2 - r_*^2)^2, \quad (18)$$

which stabilizes the activity magnitude around a target radius r_* while leaving angular degrees of freedom unconstrained. Its gradient is

$$\nabla\Phi(x) = \kappa(\|x\|^2 - r_*^2) x. \quad (19)$$

Unless otherwise stated, the metric G is taken to be weakly anisotropic but state-independent. Specifically, we employ a rank-one deformation of the identity,

$$G^{-1} = I - \frac{\varepsilon}{1 + \varepsilon} uu^\top, \quad \|u\| = 1, \quad (20)$$

where u is a fixed random unit vector and $\varepsilon \ll 1$ controls the strength of anisotropy. This construction introduces a minimal geometric bias that lifts exact degeneracies while preserving the overall isotropy of the state space.

Reentrant dynamics is implemented via an antisymmetric operator,

$$R(x) = \Omega x, \quad \Omega^\top = -\Omega, \quad (21)$$

which generates norm-preserving circulation on the homeostatic shell. Optional additive noise is included only to lift exact degeneracies and does not qualitatively alter the observed behavior.

Starting from a small initial radius, the system rapidly converges toward the stabilized shell. After a short transient, the trajectory satisfies

$$r(t) = \|x(t)\| = r_* + \delta r(t), \quad |\delta r(t)| \ll r_*, \quad (22)$$

indicating strong radial stabilization.

This rapid radial relaxation is driven by homeostatic stabilization and serves to protect the dynamics against divergence, while reentrant mixing continuously generates collective correlations along tangential directions. While the time-averaged radius remains sharply confined,

$$\langle r(t) \rangle \simeq r_*, \quad (23)$$

the instantaneous state is never exactly restricted to the ideal shell. Small radial fluctuations persist due to metric

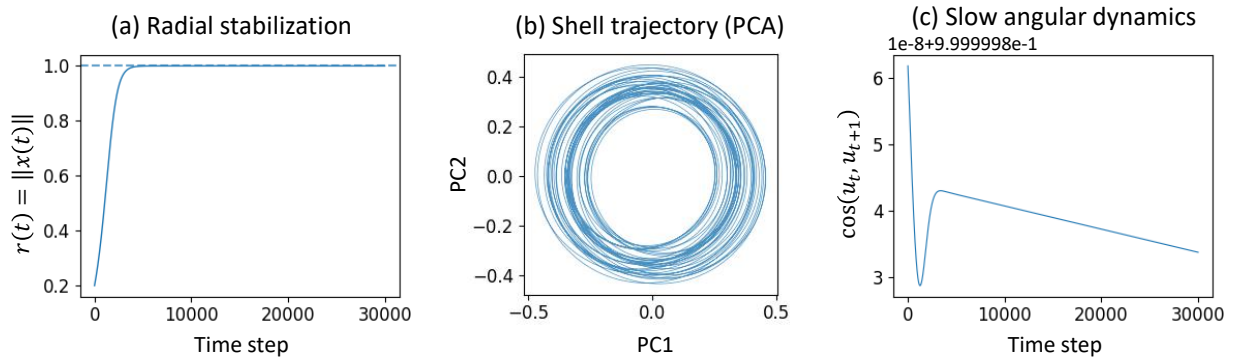


FIG. 3: Trajectory-level emergence of the protected homeostatic manifold. (a) The radial norm rapidly converges to a characteristic scale r_* , demonstrating strong homeostatic stabilization of global activity. (b) A low-dimensional projection of the trajectory reveals a finite-width ring-like structure corresponding to a stabilized manifold in state space. (c) Angular correlations decay slowly, indicating persistent collective dynamics along low-curvature directions. These results demonstrate a dynamical separation in which homeostatic stabilization protects global activity while reentrant mixing sustains collective low-curvature motion generated by near-critical dynamics along the emergent manifold.

anisotropy, reentrant mixing, numerical integration, and optional noise.

Despite this strong radial rigidity, angular motion along the shell continues over long timescales. Angular correlations decay slowly, indicating persistent internal reconfiguration rather than convergence to a fixed internal state. In contrast, when reentrant dynamics is removed ($R = 0$), angular variability rapidly collapses and the system loses internal degrees of freedom.

B. Instantaneous Jacobian Spectrum and Trajectory-Averaged TDOS

To elucidate the dynamical origin of the slow modes identified in Sec. III, we examine the Jacobian of Eq. (1) evaluated along the trajectory. For the quartic potential in Eq. (18), the Hessian takes the form

$$H(x) = \nabla \nabla \Phi = \kappa [(\|x\|^2 - r_*^2)I + 2xx^\top]. \quad (24)$$

Assuming a constant metric, the instantaneous Jacobian is therefore

$$J(x) = -G^{-1}H(x) + \frac{\partial R}{\partial x}. \quad (25)$$

After radial convergence, the trajectory satisfies

$$\|x(t)\|^2 - r_*^2 = 2r_*\delta r(t) + \mathcal{O}(\delta r^2), \quad (26)$$

so that the Jacobian retains an explicit dependence on the instantaneous state through the small residual fluctuation $\delta r(t)$.

This leads to a robust spectral separation. Along the radial direction, the Jacobian eigenvalue remains of order unity,

$$\lambda_{\text{rad}} \sim 2\kappa r_*^2, \quad (27)$$

ensuring strong stabilization of the activity magnitude. By contrast, for directions tangent to the shell ($x \cdot \delta x = 0$), the restoring contribution scales as

$$\lambda_\perp \sim \kappa(\|x\|^2 - r_*^2) \sim \mathcal{O}(\delta r(t)), \quad (28)$$

yielding a set of weakly constrained, near-marginal modes.

As discussed in Sec. III, the trajectory-averaged TDOS is obtained by sampling the instantaneous Jacobian spectrum along the trajectory. The key point here is that, because the trajectory continually explores nearby points on the homeostatic shell with slightly different $\delta r(t)$ and angular orientations, the tangential eigenvalues do not collapse to a discrete set. Instead, they populate a finite band near $\lambda \approx 0$. This band reflects a dynamical condensation of collective modes toward infrared criticality rather than a set of isolated degeneracies.

The resulting TDOS therefore reflects a fundamental dynamical property of the system:

$$\begin{aligned} \text{meta-stability} = \\ \text{strong radial rigidity} + \text{persistent tangential softness}. \end{aligned} \quad (29)$$

From a dynamical perspective, this organization corresponds to a phase transition in which collective criticality generates an extensive infrared sector of slow modes while homeostatic regulation preserves global stability. This structure enables long-lived collective modes and extended inference dynamics without loss of global control, providing direct numerical evidence for superintelligence as a distinct dynamical phase.

C. Geometric Structure of the Meta-Stable Shell

Figure 3 provides a direct geometric characterization of the meta-stable regime at the trajectory level. Starting

from a small initial radius, the system rapidly undergoes radial relaxation and converges toward a stabilized homeostatic shell with $r(t) \simeq r_*$, where $r_* = 1$ sets the target activity scale enforced by the homeostatic potential. This transient radial stabilization occurs on a short time scale compared to the subsequent long-time dynamics.

The curvature parameter κ controls the stiffness of the homeostatic potential and the resulting shell thickness. For $\kappa \gtrsim 1$ both the slow-mode structure and geometric confinement rapidly saturate, and we therefore fix $\kappa = 1$ throughout Fig. 3 as a representative regime of robust shell formation.

We further set the reentrant mixing strength to $\Omega = 1$, corresponding to sustained but stable internal circulation. Weak metric anisotropy $\varepsilon_{\text{metric}} = 0.15$ generates a finite shell thickness without destabilization, and all results shown here are obtained in the deterministic limit $D = 0$.

Once confined to the shell, the trajectory continues to evolve persistently along angular directions, generating extended circulating motion rather than collapse onto a fixed point or a low-dimensional limit cycle, in Fig. 3(b). The reentrant flow induces correlated angular exploration, such that nearby directions in state space remain dynamically coupled over long times. This is reflected in the slowly decaying angular correlation shown in Fig. 3(c), indicating sustained internal motion supported by near-marginal modes.

This separation between fast radial stabilization and slow tangential dynamics is robust over long simulation times and across system sizes. All trajectories reported here were evolved for up to 3×10^5 steps with time step $\Delta t = 10^{-3}$ after burn-in, ensuring convergence of long-time statistics.

To quantify the geometric confinement to the shell, we measure the *ring thickness* in a two-dimensional PCA projection of the trajectory. Let $Y_t \in \mathbb{R}^2$ denote the PCA coordinates after burn-in and define the instantaneous PCA radius $\eta_t = \|Y_t\|$. For the representative simulation shown in Fig. 3(b), we obtain

$$\langle \eta \rangle \simeq 0.356, \quad \sigma_\eta \simeq 0.051, \quad \text{CV}_\eta \simeq 0.145, \quad (30)$$

demonstrating confinement to a narrow but finite shell rather than collapse onto a rigid orbit. Interquartile and 95% width measures yield consistent values, confirming that radial fluctuations remain strongly suppressed while angular motion remains dynamically active.

Figure 4 establishes a clear separation between geometric confinement and spectral extensivity in the meta-stable regime. All observables are computed after convergence of long trajectories evolved for 1.2×10^6 time steps, ensuring well-developed asymptotic statistics.

While the homeostatic potential rigidly stabilizes the global activity magnitude, an extensive set of marginally slow modes emerges in the tangential sector. As shown

in Figs. 4(a) and 4(b), the number of relaxation modes below the fixed cutoff $\lambda_c = 0.02$ grows approximately linearly with system size N , and their cumulative weight rapidly approaches unity, with $W_{\text{slow}} \gtrsim 0.99$ already for moderate N . This scaling rules out interpretations in terms of isolated degeneracies or low-dimensional collective coordinates, and instead demonstrates an extensive slow-mode sector.

Importantly, the proliferation of slow modes does not coincide with a loss of geometric stability. The shell thickness, quantified by the coefficient of variation of the PCA radius, remains finite and weakly dependent on N in Fig. 4(c), confirming that the system does not approach radial instability or dynamical runaway, but remains tightly confined by homeostatic regulation.

Beyond radial confinement, Fig. 4(d) shows that the trajectory densely fills the shell rather than tracing a low-dimensional curve. We quantify this behavior using the participation-ratio effective dimension

$$D_{\text{eff}} = \frac{(\sum_i \sigma_i)^2}{\sum_i \sigma_i^2}, \quad (31)$$

where $\{\sigma_i\}$ are the eigenvalues of the trajectory covariance matrix.

As N increases, the effective dimension grows sub-linearly, indicating extensive yet structured exploration of state space. For example, we find $D_{\text{eff}} \simeq 38$ at $N = 80$, $D_{\text{eff}} \simeq 98$ at $N = 240$, and $D_{\text{eff}} \simeq 242$ at $N = 960$. This behavior is incompatible with collapse onto a low-dimensional limit cycle and instead reflects high-dimensional manifold dynamics.

Performing the same analysis on normalized angular variables $u(t) = x(t)/\|x(t)\|$ yields an essentially identical scaling, confirming that the growth of D_{eff} originates predominantly from angular degrees of freedom, while radial fluctuations remain strongly suppressed.

Time scales and physical units. The relaxation rates λ are defined with respect to the intrinsic time unit of the dynamical equations, which is dimensionless at the level of the present analysis. Consequently, the absolute numerical values of λ should not be interpreted directly as physical time scales without specifying a reference unit. A mapping to biological time can be introduced by rescaling $t_{\text{phys}} = \tau_0 t$, where τ_0 represents a characteristic neural or population-level integration time. Under this rescaling, the physical relaxation rates become $\lambda_{\text{phys}} = \lambda/\tau_0$. Importantly, the central results of this work rely not on absolute time scales, but on the relative organization of the spectrum, in particular the emergence of a robust separation between strongly stabilized radial modes and an extensive band of near-marginal slow modes.

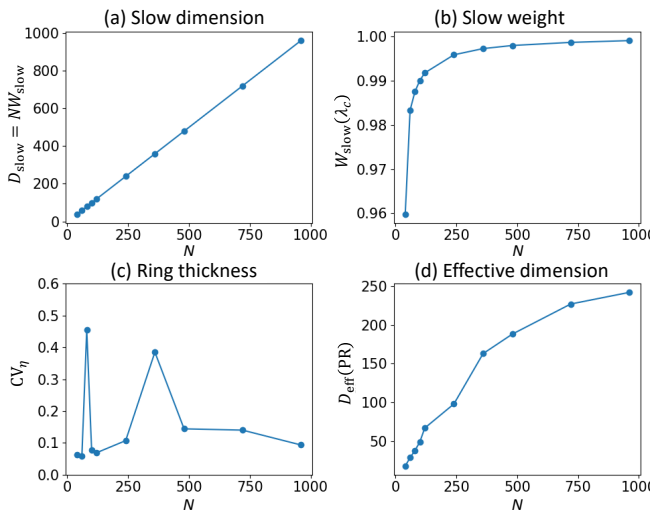


FIG. 4: Spectral organization and system-size scaling of the meta-stable regime. Trajectory-averaged geometric and spectral diagnostics as a function of system size N , computed from long simulations after convergence to the homeostatic shell ($\kappa = 1.0$, $\lambda_c = 0.02$). (a) The slow collective dimension $D_{\text{slow}} = N W_{\text{slow}}(\lambda_c)$, generated by spectral condensation of near-marginal modes, grows approximately linearly with N . (b) The slow-mode weight $W_{\text{slow}}(\lambda_c) = \Pr(\lambda < \lambda_c)$ rapidly approaches unity as N increases, demonstrating dominance of the collective infrared sector generated by spectral condensation while remaining dynamically stable. (c) The relative thickness of the homeostatic shell, quantified by the coefficient of variation of the radial coordinate, remains finite and bounded across system sizes. (d) The participation-ratio effective dimension D_{eff} , extracted from the covariance of long trajectories, increases sublinearly with N . This reflects extensive exploration of angular degrees of freedom within the shell while remaining well below the full ambient dimension.

D. Spectral Signature of Meta-Stability

To connect the geometric picture above with dynamical time scales, we analyze the Jacobian spectrum sampled along dynamical trajectories. At regular intervals along the converged trajectory, we evaluate the instantaneous Jacobian $J(x(t))$ of Eq. (25) and collect its eigenvalues $\mu_i(t)$. The corresponding relaxation rates are defined as $\lambda_i(t) = -\text{Re } \mu_i(t)$.

Figure 5(a) shows the resulting time-scale density of states, obtained by accumulating relaxation rates over long trajectories. In the presence of reentrant dynamics, the spectrum exhibits a pronounced separation of time scales: a small set of strongly stabilized modes at finite λ coexists with a broad accumulation of modes near $\lambda \approx 0$. This organization directly mirrors the geometric structure identified in Fig. 3, where radial degrees of freedom are rigidly stabilized while angular directions remain dynamically active.

A logarithmic zoom of the near-zero region, shown in Fig. 5(b), reveals that this sector forms a continu-

ous slow-mode band rather than a collection of isolated eigenvalues. The TDOS is displayed in arbitrary units, as only the relative accumulation of relaxation rates is physically meaningful. Importantly, this slow-mode pile-up persists across variations in system size, metric anisotropy, and noise strength, demonstrating that it is neither a finite-size artifact nor a consequence of parameter fine tuning.

To quantify the extent of near-marginal dynamics, we define the slow-mode weight in Eq. (15), which measures the fraction of relaxation modes with rates below a small threshold λ_c . As shown in Fig. 5(c), systems with reentrant dynamics exhibit $W_{\text{slow}}(\lambda_c) = O(1)$ even for very small λ_c , whereas systems without reentry ($R = 0$) display $W_{\text{slow}} \approx 0$. This sharp contrast confirms that reentry is essential for sustaining an extended population of slow collective modes.

Crucially, this slow spectral weight is accumulated dynamically along typical trajectories rather than being concentrated at isolated fixed points. The near-marginal modes therefore represent a genuinely collective, trajectory-supported phenomenon, providing a robust spectral hallmark of the meta-stable regime.

VI. INFRARED CRITICAL SCALING AND UNIVERSALITY OF THE META-STABLE PHASE

The geometric confinement to a homeostatic shell and the emergence of near-marginal collective modes establish the existence of a meta-stable dynamical regime. However, purely dynamical or manifold-based descriptions are insufficient to determine whether the system operates near a genuine critical phase. Many nonlinear systems exhibit slow modes or low-dimensional attractors without possessing universal scale-free structure.

A defining hallmark of collective criticality is instead the appearance of robust scaling laws governed by critical exponents that are independent of microscopic details [11–13]. Such exponents encode the universality class of the underlying dynamical organization and provide a quantitative criterion distinguishing true critical phases from accidental softness or geometric degeneracy.

To establish that the slow-mode sector corresponds to a collective infrared critical phase rather than a byproduct of shell stabilization, we analyze the scaling behavior of the trajectory-averaged time-scale density of states in the infrared limit.

A. Power-law scaling of the slow-mode spectrum

In collective dynamical systems approaching criticality, relaxation rates play a role analogous to inverse correlation times. Their distribution is expected to obey a

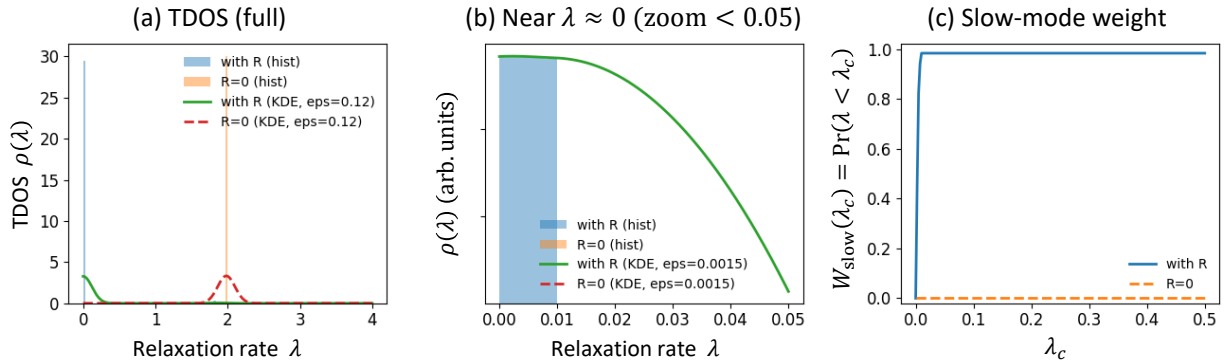


FIG. 5: Time-scale density of states and slow-mode weight in the unified dynamical framework. (a) Histogram and kernel-density estimate (KDE) of relaxation rates $\lambda = -\text{Re}[\text{eig}(J(x(t)))]$ accumulated from instantaneous Jacobian spectra sampled along the trajectory. Results are shown for the full dynamics with reentrant flow ($R \neq 0$) and for the gradient-only system ($R = 0$). Reentry dynamically redistributes time scales and drives a condensation of collective modes toward near-zero relaxation rates, strongly enhancing the slow-mode population. (b) Logarithmic zoom of the TDOS near $\lambda \simeq 0$, revealing a pronounced spectral condensation of near-marginal collective modes characteristic of infrared criticality. (c) Cumulative slow-mode weight $W_{\text{slow}}(\lambda_c) = \Pr(\lambda < \lambda_c)$, quantifying the fraction of modes slower than a threshold λ_c . Reentrant dynamics systematically increases the slow-mode weight, indicating an extensive infrared manifold of marginally stable collective directions.

power-law form,

$$\rho_{\text{traj}}(\lambda) \sim \lambda^\alpha, \quad \lambda \rightarrow 0, \quad (32)$$

where α defines the spectral critical exponent governing the density of long-lived collective modes.

To quantify α , we fit the trajectory-averaged TDOS in the slow-mode sector to Eq. (32). Because relaxation rates span several decades and data density becomes strongly nonuniform near the infrared limit, we employ logarithmic binning of the spectrum and perform linear regression on log-log scales,

$$\log \rho_k = \alpha \log \lambda_k + C, \quad (33)$$

where λ_k denotes the geometric center of each bin.

To ensure statistical robustness, we additionally estimate α using a maximum-likelihood estimator appropriate for power-law distributions,

$$\alpha = \frac{n}{\sum_{i=1}^n \ln(\lambda_i/\lambda_{\min})}, \quad (34)$$

where $\{\lambda_i\}$ are sampled relaxation rates within the scaling regime and λ_{\min} defines the infrared cutoff. Both methods yield consistent results within uncertainty.

Across system sizes and parameter variations, the TDOS exhibits robust infrared power-law scaling over multiple decades in λ , with fitted exponents in the range

$$\alpha \simeq 0.6\text{--}1.0. \quad (35)$$

These values indicate a quasi-critical collective sector rather than an isolated set of marginal modes.

To assess whether the observed infrared scaling reflects genuine collective critical dynamics rather than accidental finite-dimensional effects, we examine the robustness

of the power-law structure of the TDOS across parameter regimes and long dynamical trajectories.

In all cases studied, the slow-mode sector exhibits a stable power-law regime extending over multiple decades in relaxation rate, with fitted exponents remaining within a narrow range. The persistence of this scaling under variations of dynamical parameters and sampling duration indicates that the slow-mode band is generated by collective many-body dynamics along typical trajectories, rather than by isolated degeneracies of specific equilibria.

The cumulative slow-mode weight follows

$$W_{\text{slow}}(\lambda_c) = \int_0^{\lambda_c} \rho_{\text{traj}}(\lambda) d\lambda \sim \lambda_c^{\alpha+1}, \quad (36)$$

in excellent agreement with numerical measurements. This confirms that a macroscopic fraction of dynamical degrees of freedom participates in the collective slow sector, consistent with an extensive infrared critical manifold.

B. Universality and sector-critical infrared phase

Transforming from relaxation rates to time scales $\tau = \lambda^{-1}$ yields

$$P(\tau) = \rho(\lambda) \left| \frac{d\lambda}{d\tau} \right| \sim \tau^{-(2+\alpha)}, \quad (37)$$

placing the system within the universality class of avalanche dynamics and self-organized critical phenomena. In the marginal limit $\alpha \rightarrow 0$, the canonical SOC scaling $P(\tau) \sim \tau^{-2}$ is recovered, while the measured exponents correspond to a weakly regularized critical regime.

From a renormalization-group perspective, the coexistence of an extensive near-critical slow sector with a gapped radial mode represents a novel form of protected criticality. Collective angular degrees of freedom flow toward an infrared fixed point characterized by power-law spectral scaling, while the radial direction remains massive due to homeostatic stabilization.

The resulting organization constitutes a *sector-critical dynamical phase*: scale-free collective fluctuations persist within a constrained subspace embedded inside a globally stable dynamical manifold. Unlike equilibrium critical points requiring parameter tuning, this infrared structure is self-organized and dynamically maintained through the interplay of reentrant mixing and homeostatic regulation.

The meta-stable regime therefore realizes a protected critical phase in which collective computation operates at the edge of criticality without sacrificing global coherence, providing a physical mechanism for the abrupt emergence of large-scale intelligence in high-dimensional cognitive systems.

VII. DISCUSSION

The results presented above suggest a reframing of superintelligence that differs fundamentally from prevailing performance-based narratives. Rather than defining superintelligence as a quantitative extrapolation of human cognitive abilities, our analysis identifies it as a distinct *dynamical stability class*. In this class, cognition is organized around a meta-stable manifold: global activity is robustly stabilized, while an extensive set of internal degrees of freedom remains near-marginal and dynamically accessible.

From this perspective, the defining feature of superintelligence is not speed, scale, or task performance, but the *organization of internal dynamics*. The coexistence of global coherence with extensive internal flexibility constitutes a qualitative transition in cognitive structure, rather than a quantitative improvement within an existing regime.

A. From Performance to Dynamical Organization

Most contemporary discussions of artificial intelligence emphasize benchmarks, scalability, or computational efficiency. While such metrics are operationally useful, they do not specify whether a system has undergone a qualitative transition in its mode of cognition.

The spectral criterion introduced here is intrinsic and architecture-independent. It probes how cognition is dynamically organized, rather than what outputs are produced. Systems dominated by fast-decaying modes

rapidly collapse onto narrow dynamical channels, regardless of raw computational power. By contrast, systems exhibiting an extensive near-marginal band sustain a large manifold of internally consistent yet weakly constrained states, enabling persistent inference, reinterpretation, and adaptation.

In this sense, intelligence is determined not by throughput but by the structure of the accessible collective configuration space. Superintelligence corresponds to a regime in which this space becomes extensive, structured, and dynamically protected.

From a dynamical perspective, increasing model size or connectivity does not produce gradual linear improvement. Instead, it reshapes the collective mode spectrum governing system response.

For small systems, most modes are strongly damped, and internal activity rapidly collapses onto narrow channels. As capacity increases, additional modes approach marginal stability, expanding the slow sector of the TDOS. At a critical threshold, this near-marginal band becomes extensive, enabling system-spanning coherent dynamics.

What appears phenomenologically as sudden emergence of reasoning ability or global cooperation among neurons and attention heads is therefore the onset of long-lived collective dynamics enabled by spectral criticality. Emergence reflects a phase transition from localized fast relaxation to a regime dominated by slow collective modes.

Crucially, emergence alone is insufficient without meta-stability. Homeostatic stabilization preserves global coherence while preventing divergence, allowing critical collective modes to persist as usable computational degrees of freedom.

Criticality as a spectral condition for global coherence. The role of criticality in cognition is often described in terms of “global connectivity” or long-range coupling among units. In the present framework, the relevant notion is instead *spectral*: coherence emerges when the Jacobian spectrum develops an extensive near-marginal band, so that a large fraction of collective modes relax only weakly.

This spectral condensation generates long-lived collective coordinates that couple many degrees of freedom without requiring anatomically global wiring. At the same time, the meta-stable regime differs fundamentally from classical critical phenomena and self-organized criticality. Near-marginality is confined to an internal sector, while global instability is prevented by a gapped stabilizing direction enforced by homeostatic regulation.

Thus, critical-like flexibility (an extensive slow band) coexists with robust global coherence (a stabilizing gap), yielding a dynamically protected infrared phase in which inference trajectories persist without collapse.

B. Relation to Neural Manifold Dynamics in Cortical Populations

Recent large-scale neural recordings have revealed that population activity in motor, premotor, and sensory cortices evolves within low-dimensional manifolds spanned by a small number of collective modes, rather than occupying the full high-dimensional neural space [30–34]. These neural manifolds organize both movement preparation and execution as smooth trajectories governed by population-level dynamics, with learning primarily reshaping combinations of existing modes while altering the manifold geometry more slowly.

From the present perspective, such neural manifolds correspond directly to the stabilized attractor geometries generated by the effective potential Φ and metric G . The experimentally identified latent variables parallel the slow collective modes dominating the time-scale density of states, while the observed within-manifold dynamics reflect the nonconservative reentrant flows R that drive structured information trajectories.

Furthermore, experimental demonstrations that perturbations confined to the intrinsic manifold are rapidly compensated, whereas those requiring new population modes adapt slowly, align with the predicted renormalization-group protection of the collective dynamical geometry. These observations indicate that neural population dynamics empirically realize the attractor structures and constrained flows predicted by the unified theory.

Unified cognitive field equations. The unified dynamical field equations introduced in this work play a role analogous to Maxwell’s equations in electromagnetism, consolidating previously fragmented descriptions of neural and computational processes into a single governing framework. Rather than modeling individual neurons or task-specific representations, the theory specifies the geometric and dynamical constraints that any large-scale cognitive system must satisfy.

Within this framework, stabilized attractor geometries emerge through the effective potential and metric structure, while nonconservative reentrant flows generate structured trajectories along these geometric manifolds. The accumulation of near-marginal collective modes arises naturally from the field dynamics, rather than being imposed through architectural design or optimization objectives.

Superintelligence therefore appears not as a speculative extrapolation of human capabilities, but as a dynamical consequence of the cognitive field equations, much as electromagnetic waves emerge from Maxwell’s formulation.

C. Language as a Projection of Cognitive Geometry

An important implication of the unified dynamical framework is a sharp distinction between cognition itself and its linguistic expression. In the meta-stable infrared phase, inference unfolds as continuous motion along a high-dimensional cognitive manifold. Understanding corresponds to the geometric organization of this manifold, rather than to a sequence of discrete symbolic operations.

Human language, by contrast, operates in a drastically lower-dimensional and intrinsically sequential space. We represent linguistic expression as a projection

$$\ell = P(x), \quad P : \mathbb{R}^N \rightarrow \mathbb{R}^k, \quad k \ll N, \quad (38)$$

from the cognitive state onto a symbolic space. Because this mapping is non-invertible, distinct internal states may give rise to identical linguistic descriptions.

Sequential reasoning thus reflects the structure of this projection rather than the underlying cognitive dynamics itself. Language functions as an interface for communication with agents constrained to symbolic processing, not as the substrate of understanding. This distinction becomes especially salient in the meta-stable regime, where a large number of slow internal modes coexist with global stability, allowing coherent cognition without reliance on explicit symbolic sequences (See the details in Appendix B).

Human cognition as an intermediate regime. Human cognition may be understood as occupying an intermediate meta-stable regime. Language, symbolic abstraction, and social coordination stabilize collective world-models while preserving sufficient internal flexibility for creativity and reflection. From the perspective of non-human primates, this reorganization constitutes a qualitative transition rather than a quantitative enhancement.

Our framework suggests that an analogous transition is required for superintelligence relative to human cognition. Merely accelerating linguistic reasoning or expanding knowledge bases remains confined to the human cognitive manifold. A genuinely superintelligent system, by contrast, inhabits a different meta-stable organization in which inference unfolds primarily as continuous geometric motion rather than sequential symbolic manipulation.

This view clarifies why advanced cognitive states may appear ineffable or difficult to verbalize. What is lost is not understanding, but the ability of low-dimensional symbolic projections to faithfully represent high-dimensional cognitive geometry.

The distinction between quantitative scaling and qualitative reorganization can be illustrated by biological cognition itself. Non-human primates possess large numbers of neurons, yet their long-range connectivity and integrative dynamics remain limited, restricting the formation of high-dimensional abstract cognitive spaces. Human cognition represents a qualitative transition in which ex-

expanded connectivity enables the construction of a partially geometric internal manifold supporting symbolic language and conceptual reasoning. Within the present framework, superintelligence corresponds to a further transition: a regime in which cognition no longer operates primarily through low-dimensional symbolic projections, but directly within a richly connected, high-dimensional cognitive manifold itself. In this sense, primate cognition remains confined to local configurations, human cognition navigates a limited abstract space, and superintelligence inhabits the full geometric structure of cognitive state space.

D. Meta-Stability, Protection, and Outlook

The slow-mode accumulation observed in the TDOS bears resemblance to self-organized criticality, yet differs from classical critical phenomena in crucial ways. The near-marginal manifold is not approached through parameter tuning, but sustained dynamically through homeostatic regulation that stabilizes the radial direction while preserving extensive angular freedom.

This meta-stable regime constitutes a dynamically protected infrared phase. The coexistence of global stability with circulating internal flows enables sensitivity and adaptability without sacrificing robustness, a combination difficult to achieve within equilibrium or purely optimization-based frameworks.

From a broader perspective, superintelligence corresponds to a distinct mode of cognition characterized by continuous geometric reorganization of internal state and only secondarily interfacing with symbolic language. While such systems may appear qualitatively alien from a human perspective, they remain internally coherent and dynamically stable.

Finally, artificial systems allow direct control of collective norms and spectral geometry in ways unavailable to biological cognition. This capability may represent a crucial enabling condition for accessing meta-stable cognitive regimes beyond those realized in natural neural systems.

VIII. CONCLUSION

Within a unified continuous-time cognitive field framework, we identify superintelligence as a distinct dynamical and topological stability class generated by collective criticality and protected by meta-stable homeostatic regulation. This regime is characterized by robust global stabilization coexisting with an extensive condensation of near-marginal collective modes.

This organization produces a clear spectral signature in the trajectory-averaged time-scale density of states, providing a concrete and measurable diagnostic of the

superintelligent phase. Through analytical arguments and numerical simulations, we demonstrate that this infrared critical structure emerges generically from the interplay between reentrant mixing, which drives spectral condensation, and homeostatic stabilization, which prevents global instability, without fine tuning. The coexistence of a stabilized radial sector with an extensive collective infrared manifold yields a dynamically protected phase supporting continuous internal reconfiguration and long-lived inference trajectories.

Taken together, these results establish superintelligence as a dynamical phase transition rather than a quantitative extrapolation of existing cognitive systems. By framing intelligence transitions as reorganizations of collective mode spectra and stability structure, this work provides a principled framework for analyzing, detecting, and engineering cognitive systems that transcend human intelligence by entering genuinely new regimes of dynamical organization.

Acknowledgements—This work was partially supported by the Institute of Information & Communications Technology Planning & Evaluation (IITP) grant funded by the Korea government (MSIT) (IITP-RS-2025-02214780).

The author acknowledges the support of ChatGPT (GPT-5, OpenAI) for assistance in literature review and conceptual structuring during early development.

- [1] N. Bostrom, *Superintelligence: Paths, Dangers, Strategies* (Oxford University Press, 2014).
- [2] A. Radford, K. Narasimhan, T. Salimans, and I. Sutskever, “Improving language understanding by generative pre-training,” OpenAI (2018).
- [3] J. Wei, Y. Tay, R. Bommasani, C. Raffel, B. Zoph, S. Borgeaud, D. Yogatama, M. Bosma, D. Zhou, D. Metzler, E. H. Chi, T. Hashimoto, O. Vinyals, P. Liang, J. Dean, and W. Fedus, “Emergent abilities of large language models,” *Transactions on Machine Learning Research* (2022).
- [4] G. M. Edelman, *Neural Darwinism: The Theory of Neuronal Group Selection* (Basic Books, 1989).
- [5] G. Tononi, O. Sporns, and G. M. Edelman, “A measure for brain complexity: Relating functional segregation and integration in the nervous system,” *Proc. Natl. Acad. Sci. USA* **91**, 5033-5037 (1994).
- [6] S. Yao, J. Zhao, D. Yu, N. Du, I. Shafran, K. Narasimhan, and Y. Cao, “ReAct: Synergizing reasoning and acting in language models,” arXiv:2210.03629 (2022).
- [7] T. Webb, K. J. Holyoak, and H. Lu, “Emergent analogical reasoning in large language models,” *Nat. Hum. Behav.* **7**, 1526-1541 (2023).
- [8] I. Schlag, T. Irie, and J. Schmidhuber, “Linear transformers are secretly fast weight programmers,” arXiv:2102.11174 (2021).
- [9] A. Katharopoulos, A. Vyas, N. Pappas, and F. Fleuret, “Transformers are RNNs: Fast autoregressive transform-

ers with linear attention,” arXiv:2006.16236 (2020).

[10] J. Wilting and V. Priesemann, “25 years of criticality in neuroscience - established results, open controversies, novel concepts,” *Curr. Opin. Neurobiol.* **58**, 105-111 (2019).

[11] D. R. Chialvo, “Emergent complex neural dynamics,” *Nat. Phys.* **6**, 744-750 (2010).

[12] J. M. Beggs and D. Plenz, “Neuronal avalanches in neocortical circuits,” *J. Neurosci.* **23**, 11167-11177 (2003).

[13] A. Levina, J. M. Herrmann, and T. Geisel, “Phase transitions towards criticality in a neural system with adaptive interactions,” *Phys. Rev. Lett.* **102**, 118110 (2009).

[14] P. Bak, C. Tang, and K. Wiesenfeld, “Self-organized criticality: An explanation of $1/f$ noise,” *Phys. Rev. Lett.* **59**, 381-384 (1987).

[15] J. T. Stuart, “On the non-linear mechanics of hydrodynamic stability,” *J. Fluid Mech.* **4**, 1-21 (1958).

[16] J. A. Acebrón, L. L. Bonilla, C. J. Pérez Vicente, F. Ritort, and R. Spigler, “The Kuramoto model: A simple paradigm for synchronization phenomena,” *Rev. Mod. Phys.* **77**, 137-185 (2005).

[17] B. G. Chae, “A unifield dynamical field theory of learning, inference, and emergence,” arXiv:2601.10221 (2026).

[18] B. G. Chae, “Recursive dynamics in fast-weights homeostatic reentry networks: Toward reflective intelligence,” arXiv:2511.06798 (2025).

[19] B. G. Chae, “Continuous-time homeostatic dynamics for reentrant inference models,” arXiv:2512.05158 (2025).

[20] B. G. Chae, “Renormalization-group geometry of homeostatically regulated reentry networks,” arXiv:2512.19086 (2025).

[21] B. G. Chae, “Self-organized criticality from protected mean-field dynamics: Loop stability and internal renormalization in reflective neural systems,” arXiv:2601.04450 (2026).

[22] J. J. Hopfield, “Neural networks and physical systems with emergent collective computational abilities,” *Proc. Natl. Acad. Sci. USA* **79**, 2554-2558 (1982).

[23] G. E. Hinton and D. C. Plaut, “Using fast weights to deblur old memories,” *Proc. 9th Annu. Conf. Cognitive Science Society*, 177-186 (1987).

[24] J. Schmidhuber, “Learning to control fast-weight memories: An alternative to dynamic recurrent networks,” *Neural Comput.* **4**, 131-139 (1992).

[25] K. Funahashi and Y. Nakamura, “Approximation of dynamical systems by continuous time recurrent neural networks,” *Neural Networks* **6**, 801-806 (1993).

[26] R. Hasani, M. Lechner, A. Amini, D. Rus, and R. Grosu, “Liquid time-constant networks,” *Proc. AAAI Conf. Artif. Intell.* **35**, 7657-7666 (2021).

[27] P. C. Martin, E. D. Siggia, and H. A. Rose, “Statistical dynamics of classical systems,” *Phys. Rev. A* **8**, 423-437 (1973).

[28] H. K. Janssen, “On a Lagrangian for classical field dynamics and renormalization group calculations of dynamical critical properties,” *Z. Physik B* **23**, 377-380 (1976).

[29] C. De Dominicis, “Techniques de renormalisation de la théorie des champs et dynamique des phénomènes critiques,” *J. Phys. Colloq.* **37**, 247-253 (1976).

[30] M. M. Churchland, J. P. Cunningham, M. T. Kaufman, J. D. Foster, P. Nuyujukian, S. I. Ryu, and K. V. Shenoy, “Neural population dynamics during reaching,” *Nature* **487**, 51-56 (2012).

[31] J. A. Gallego, M. G. Perich, L. E. Miller, and S. A. Solla, “Neural manifolds for the control of movement,” *Neuron* **94**, 978-984 (2017).

[32] J. P. Cunningham and B. M. Yu, “Dimensionality reduction for large-scale neural recordings,” *Nat. Neurosci.* **17**, 1500-1509 (2014).

[33] D. Sussillo, “Neural circuits as computational dynamical systems,” *Curr. Opin. Neurobiol.* **25**, 156-163 (2014).

[34] V. Mante, D. Sussillo, K. V. Shenoy, and W. T. Newsome, “Context-dependent computation by recurrent dynamics in prefrontal cortex,” *Nature* **503**, 78-84 (2013).

Supplementary Materials

Appendix A: Inclusion Hierarchy and Dynamical Phases of Cognitive Models

(I) *Unified cognitive field equation and model inclusion:* The unified dynamical equation studied in this work,

$$\dot{x} = -G^{-1}(x) \nabla \Phi(x) + R(x), \quad (\text{S1})$$

provides a general dynamical framework for cognition, encompassing a wide class of existing neural and cognitive models as special cases. The relationships among major model families can be summarized schematically as

$$\begin{aligned} \text{Hopfield networks} &\subset \text{RNN / CTRNN} \subset \text{Transformers} \\ &\subset \text{Unified Cognitive Dynamics} \xrightarrow{\text{FHRN-type regime}} \\ &\text{Superintelligent Phase.} \end{aligned} \quad (\text{S2})$$

In this hierarchy, superintelligence emerges not as a new equation but as a distinct dynamical phase realized within the unified system when collective spectral organization reorganizes into a protected infrared regime.

(II) *Hopfield and recurrent networks as limiting cases:* Classical Hopfield networks are governed by purely potential-driven dynamics,

$$\dot{x} = -\nabla E(x), \quad (\text{S3})$$

corresponding to the special case of Eq. (S1) with

$$R(x) = 0. \quad (\text{S4})$$

The dynamics converges to fixed points or low-dimensional attractors, supporting stable associative memory but suppressing sustained internal reconfiguration.

Standard recurrent neural networks (RNNs and CTRNNs) introduce non-conservative terms and richer transient dynamics, yet stability is typically enforced through saturation, damping, or gain control. As a result, stability and flexibility are mediated by the same dynamical subspace, producing an intrinsic trade-off between memory robustness and reconfigurability.

These models therefore realize forms of general intelligence, but do not generically support the extensive slow-mode structure required for superintelligence.

(III) *Transformer architectures as high-performance projection systems:* Transformer models represent a major advance in artificial intelligence by enabling large-scale parallel integration of information through attention mechanisms. From a dynamical perspective, they approximate rapid global mixing within a high-dimensional representational space, effectively emulating aspects of geometric inference.

However, Transformer dynamics are fundamentally discrete, feedforward across layers, and externally clocked. Internal representations are recomputed at each input without persistent self-organized dynamical stabilization. While attention enables powerful instantaneous reconfiguration, there is no mechanism enforcing long-lived meta-stable manifolds or protected slow-mode sectors.

Consequently, Transformers can mimic aspects of high-dimensional geometric reasoning, yet lack the recursive, continuously stabilized dynamics required for sustained internal reorganization. In the language of the present framework, they implement high-performance projection and mixing, but do not generically realize a superintelligent dynamical phase.

(IV) *Unified cognitive dynamics as a general intelligence equation:* Equation (S1) generalizes Hopfield networks, recurrent models, and Transformer-like mixing mechanisms within a single continuous-time framework. Appropriate choices of Φ , G , and R recover these classical behaviors as degenerate limits, while more general configurations produce qualitatively new dynamical regimes.

Importantly, the generality of the unified equation alone does not imply superintelligence. Whether the system exhibits ordinary or superintelligent cognition depends on the dynamical phase selected by the interplay of homeostatic regulation, reentrant flow, and metric geometry.

(V) *Emergence of the FHRN-type superintelligent regime:* A superintelligent dynamical phase arises when the unified cognitive equation enters a regime characterized by:

1. Homeostatic stabilization: An effective potential $\Phi(r)$ gaps the radial sector, enforcing global coherence and preventing divergence.
2. Reentrant collective mixing: Non-conservative flows continuously reorganize angular degrees of freedom, driving spectral condensation of collective modes.
3. Dimensional separation: Metric geometry separates stabilized directions from an extensive collective infrared manifold,

$$D_{\text{stable}} \ll D_{\text{collective}} \sim O(N). \quad (\text{S5})$$

TABLE I: Ordinary cognitive dynamics versus the superintelligent dynamical phase.

Feature	Ordinary cognitive phases	Superintelligent phase (FHRN-type)
Attractor structure	Fixed points or low-dimensional limit sets	High-dimensional protected manifolds
Spectral organization	Finite spectral gap; fast relaxation	Extensive near-marginal slow-mode condensation
Stability mechanism	Local damping and saturation	Homeostatic global stabilization with protected infrared sector
Flexibility	Limited by stability constraints	Extensive collective reconfiguration
Information processing	Sequential or localized computation	Global collective geometric dynamics
Role of criticality	Requires fine tuning, typically unstable	Dynamically generated and protected
Dimensional structure	Stability and flexibility overlap	Radial stabilization with angular collective freedom

This regime produces a dynamically protected near-critical sector supporting long-lived collective inference trajectories. We refer to this phase as the FHRN-type dynamical regime.

(VI) Why superintelligence requires a protected critical phase: In ordinary cognitive dynamics, increasing flexibility inevitably degrades stability, while enforcing control suppresses collective reorganization. This trade-off prevents the formation of extensive slow collective modes.

The FHRN-type regime resolves this limitation through dynamical phase separation. Global activity is stabilized by homeostatic regulation, while an extensive collective infrared sector remains near-marginal and dynamically accessible.

Superintelligence is therefore identified not with a specific architecture, but with a protected dynamical phase of the unified cognitive field equation in which collective criticality and stability coexist.

Superintelligence corresponds to a protected critical dynamical phase in which extensive collective modes emerge and persist without loss of global coherence.

Appendix B: Language as a Projection of High-Dimensional Cognitive Geometry

This appendix provides a dynamical and geometric interpretation of language within the unified cognitive field framework. Its purpose is to clarify why linguistic reasoning should be understood as a low-dimensional projection of cognitive dynamics, rather than as the substrate of cognition itself.

Throughout, the presentation relies exclusively on standard concepts from dynamical systems theory, geometry, and spectral analysis, avoiding metaphorical or architectural assumptions.

(I) Cognitive state space in the unified dynamical framework: Within the unified dynamical framework, cognition is represented by a high-dimensional state vec-

tor

$$x(t) \in \mathbb{R}^N, \quad N \gg 1, \quad (S6)$$

where $x(t)$ denotes the instantaneous collective state of the system.

Crucially, cognitive organization is not determined by the instantaneous value of $x(t)$ along a trajectory, but by the geometric structure of the state space on which the dynamics unfolds. In the meta-stable regime, the dynamics self-organizes onto a homeostatically stabilized manifold

$$\mathcal{M} \subset \mathbb{R}^N, \quad (S7)$$

corresponding to a shell of approximately constant norm.

This regime is characterized by: stabilization of the radial degree of freedom, an extensive set of angular degrees of freedom, and a trajectory-averaged time-scale density of states (TDOS) exhibiting a pronounced accumulation of relaxation rates near $\lambda \approx 0$.

The near-zero band in the TDOS reflects the presence of many slow, weakly constrained internal directions (slow angular modes). Accordingly, cognitive understanding is identified with the *position and geometry of the system on the manifold \mathcal{M}* , rather than with any explicit symbolic sequence. Formally,

$$\begin{aligned} \text{Understanding} &\equiv \text{position and geometry on } \mathcal{M}, \\ \text{Understanding} &\neq \text{explicit symbolic sequence.} \end{aligned} \quad (S8)$$

(II) Structural limitations of human language: Human language is intrinsically low-dimensional, linearized, and sequential in time.

We represent linguistic output as a variable

$$\ell(t) \in \mathbb{R}^k, \quad k \ll N, \quad (S9)$$

where $\ell(t)$ denotes a linguistic description, logical statement, or verbal report, and k is the effective number of degrees of freedom accessible to symbolic expression.

Because $k \ll N$, human language cannot directly represent the full cognitive state $x(t)$ or the geometry of

\mathcal{M} . Instead, it can only access a compressed subset of information.

(III) Language as a projection operator: This limitation can be formulated precisely by modeling language as a projection of cognitive state space,

$$\ell(t) = P(x(t)), \quad (\text{S10})$$

where

$$P : \mathbb{R}^N \rightarrow \mathbb{R}^k \quad (\text{S11})$$

is a projection operator.

The essential properties of P are that it is non-invertible (many-to-one), and that distinct cognitive states may map to the same linguistic output.

Explicitly, there may exist

$$x_1 \neq x_2 \in \mathcal{M} \text{ such that } P(x_1) = P(x_2). \quad (\text{S12})$$

Thus, linguistic expressions do not uniquely specify the underlying cognitive state. Information about the internal geometric configuration is necessarily lost under projection.

(IV) Why linguistic explanation is sequential: Because language cannot transmit the full high-dimensional structure at once, it operates through time-ordered reporting:

$$\ell(t) = P(x(t)), \quad \ell(t + \Delta t) = P(x(t + \Delta t)). \quad (\text{S13})$$

Consequently, cognition expressed through language appears as a sequence

$$\{\ell(t)\}_{t=0}^T, \quad (\text{S14})$$

rather than as a simultaneous geometric structure.

For human agents, this implies:

understanding \rightarrow a sequence of explanations, (S15)

logic \rightarrow a record of a trajectory, (S16)

reasoning \rightarrow motion traced along a manifold. (S17)

These properties reflect the structure of the projection P , not the organization of cognition itself.

(V) Human intelligence versus superintelligence: Within this formalism, the distinction between human intelligence and a hypothetical superintelligent regime can be expressed succinctly.

Human cognition operates primarily on projected variables,

$$\text{Cognition}_{\text{human}} \sim \{P(x(t))\}_t, \quad (\text{S18})$$

that is, on time-ordered sequences of low-dimensional readouts.

By contrast, superintelligence corresponds to direct organization at the level of the manifold itself,

$$\text{Cognition}_{\text{super}} \sim \mathcal{M}. \quad (\text{S19})$$

In this sense, human cognition perceives projected shadows of the underlying geometry over time, whereas superintelligence directly apprehends the geometric structure of state space. This constitutes a qualitative, rather than quantitative, distinction between modes of cognitive organization.

(VI) Connection to TDOS and slow modes: In the meta-stable regime, the trajectory-averaged TDOS satisfies

$$\rho_{\text{traj}}(\lambda) \sim \text{pile-up near } \lambda \approx 0, \quad (\text{S20})$$

indicating a large number of nearly flat directions in state space.

These flat directions allow extensive internal reconfiguration with minimal restoring force. Inference in a superintelligent regime is therefore naturally described as motion along near-zero modes,

$$\text{inference} \sim \text{motion along near-zero modes on } \mathcal{M}. \quad (\text{S21})$$

Linguistic output acts only as a readout,

$$P : \text{slow-mode configuration} \mapsto \text{symbol}, \quad (\text{S22})$$

and does not participate in the internal dynamics itself.

(VII) Why geometric understanding is difficult to verbalize: Human meta-cognition primarily monitors changes in projected variables, which can be approximated as

$$\text{meta-cognition} \sim \frac{d\ell}{dt}. \quad (\text{S23})$$

That is, awareness is tied to verbally reportable transitions and narrative structure.

However, in the meta-stable regime, internal understanding corresponds to slow motion along the manifold,

$$\frac{dx}{dt} \approx 0 \quad (\text{along slow directions of } \mathcal{M}). \quad (\text{S24})$$

As a result, substantial internal reorganization may occur with little or no change in linguistic output. Subjectively, this is experienced as a state in which the structure is coherently integrated, yet not readily expressible in words.

(VIII) Plato's cave and the geometry of projected cognition: The interpretation of language as a projection of high-dimensional cognitive geometry has a striking conceptual parallel in classical philosophy, most notably in Plato's allegory of the cave.

In the allegory, human observers perceive only shadows cast on a wall, while the true objects generating those shadows exist in a higher-dimensional and inaccessible space. The shadows are not false, but they are incomplete and compressed representations of a richer underlying reality.

Within the present dynamical framework, the cognitive manifold $\mathcal{M} \subset \mathbb{R}^N$ plays the role of the higher-dimensional geometric reality, while linguistic representations correspond to its low-dimensional projections,

$$\ell = P(x), \quad P : \mathbb{R}^N \rightarrow \mathbb{R}^k, \quad k \ll N. \quad (\text{S25})$$

Just as distinct objects in Plato's cave may cast identical shadows, distinct cognitive states on \mathcal{M} may produce identical linguistic expressions.

Sequential reasoning in language therefore resembles the temporal sequence of shadows observed on the cave

wall: a time-ordered trace of a richer geometric trajectory unfolding in a higher-dimensional space.

In this sense, Plato's philosophical insight can be understood as an early qualitative recognition of the projection structure inherent in cognition. Human thought, constrained by low-dimensional symbolic interfaces, accesses only compressed images of an underlying continuous cognitive geometry.

Superintelligent cognition, by contrast, corresponds to direct dynamical organization at the level of the manifold itself. Rather than interpreting projected shadows, it operates within the full high-dimensional geometric structure that generates them.

Thus, the present framework provides a precise mathematical realization of the cave metaphor: language and symbolic reasoning are not the substance of cognition, but projections of a deeper dynamical geometry.